Atomic Scattering from Single Adsorbates: What Can We Learn from the Gas Phase?

Didier Lemoine*

Laboratoire de Dynamique Moléculaire et Photonique, URA CNRS 779, Centre d'Etudes et de Recherches Laser et Applications,† Université de Lille 1, Bâtiment P5, 59655 Villeneuve d'Ascq Cedex, France

(Received 11 February 1998)

Numerically exact studies of atomic scattering from single adsorbates on a flat surface are based on a soft potential closely approximating a hemisphere geometry, and on the ideal, hard and soft hemisphere models. The hard wall model cannot fit any of the five interference maxima of the angular distribution. In contrast, the soft hemisphere model perfectly predicts the first three interference peaks. Moreover, the first interference peak is revealed as the well-known gas phase rainbow arising from the van der Waals interaction between the scatterer and the adsorbate. [S0031-9007(98)06531-4]

PACS numbers: 79.20.Rf, 34.10.+x, 34.50.Dy

In the context of gas phase collisions the angular dependence of the differential cross section is well characterized [1,2]. The classical rainbow singularity and the quantal diffraction process give rise to pronounced oscillatory interference patterns. The resulting structure can be traced to the scatterer-target interaction and accurate potential energy surfaces can be inverted from beam scattering data [1–3], at least for closed-shell systems. When one collision partner is a molecule the main effect of the orientational anisotropy is the damping of the oscillations, whereas the diffraction spacing is primarily determined by the isotropic potential [3,4]. One basic question to be addressed in this study is the following: What do we know from gas phase scattering that can be transferred to the situation in which the atomic or molecular target is adsorbed on a smooth surface?

In the past decade Toennies and co-workers have succeeded in characterizing the angular distributions of helium atoms scattering from isolated CO adsorbates on smooth metal surfaces [5–7]. They have measured the scattered beam intensities that are analogous to the differential cross sections in gas phase collisions. One can then expect both diffraction and rainbow effects to occur [8,9]. In addition, collisions with both the adsorbate and the metal surface combine with the direct scattering from the adsorbate in order to give rise to the so-called reflection symmetry interferences [7]. Next, the energy transfer with surface phonons or with hindered modes of the adsorbed molecule must be accounted for. Toennies and co-workers have checked that the scattering was dominated by the elastic signal owing to a time-of-flight analysis [5–7]. Hence, the interpretation of the observed interference patterns can be based on a rigid adsorbate + surface system, further assuming a flat surface since the CO-induced corrugation is much larger than that of the smooth surface.

Many attempts have been made to explain the resulting oscillatory structures in terms of an ideal hard wall interaction model consisting of a hemisphere lying on a flat surface [5–7,10–12]. The intuitive nature and the easy dynamical resolution implied by such a simple interaction model clearly contribute to its attractiveness and popularity. The physics contained in the hard hemisphere model involves diffraction processes and reflection symmetry interferences. However, it lacks in any distortion of these mechanisms as well as rainbow effects, due to the neglect of the attractive range and of inflection points in the repulsive wall of the realistic He + defect/surface interaction potential [8,9]. The limited applicability of the hard wall model shows up in the fact that the apparent adsorbate radius cannot be expected to increase from a reasonable value of 2.4 Å (i.e., comparable to the gas phase radius) at the collision energy $E_i = 40.3$ meV, up to 4.4 Å at $E_i = 9.4$ meV, as given by the best fit calculations of Choi, Tang, and Toennies [11].

In closing the introductory section it is worth noting that an exact dynamical resolution is required in order to determine accurately the positions of the intensity maxima, which constitute the useful information to confront with experimental data [5–7,11]. Indeed, all kinds of scattering approximations, including classical, semiclassical, sudden, and reduced dimensionality treatments, have already been applied but none can be found to yield satisfactory fits to the angular distributions, either experimental [11] or stemming from the exact, three-dimensional (3D) quantum calculations of Carré and Lemoine (CL) [9]. Therefore, the present study relies exclusively on the exact solution of the Schrödinger equation for the motion of the atomic scatterer. Two simplified interaction models are investigated and tested against the 3D scattering calculations of CL, based on a soft potential closely approximating a hemisphere geometry as depicted in Fig. 1. One is the hard hemisphere lying on the flat surface, and the other will be termed the soft hemisphere model, upgrading the hard sphere potential to a realistic isotropic interaction between the scatterer and the adsorbate. The highlights of the investigation are twofold: (1) The adequacy of the hard hemisphere model is denied, and, most importantly, (2) the exact angular distribution is now fully characterized; i.e., every intensity peak is assigned with respect to the analogous gas phase diffraction or rainbow feature, or to a surface-specific interference effect.

 © 1998 The American Physical Society

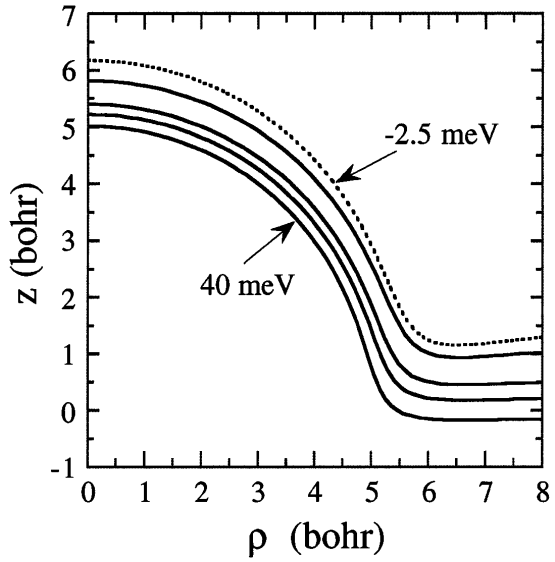

FIG. 1. Potential energy contours for He scattering from CO adsorbed on Pt(111) in a plane perpendicular to the surface. Solid equipotentials are repulsive (0, 10, 20, 40 meV), whereas the dashed one is for −2.5 meV.

The scattered intensity or differential cross section is defined by the square of the scattering amplitude [1,2,12]. By assuming a hemisphere lying on a flat surface the atomic scattering from a single adsorbate can be formulated as the difference of two gas phase collision events, enforcing the proper boundary conditions along the mirror plane by symmetry [13–15]. These are determined by reflection construction and involve the free sphere obtained by extending the adsorbed hemisphere by symmetry [14]. One can then express the scattering amplitude for the adsorbed hemisphere model, F, in terms of those for the free sphere, f, such as

$$F(\mathbf{k}_f, \mathbf{k}_i) = f(\mathbf{k}_f \cdot \mathbf{k}_i) - f(\mathbf{k}_f \cdot \mathbf{k}_s), \qquad (1)$$

where $\mathbf{k}$ is a wave vector and the indices, i, f, and s denote the incident, final, and specular directions, respectively. The first amplitude describes the direct scattering from the adsorbate with incident wave vector $\mathbf{k}_i$, whereas the second contribution represents the waves specularly reflected from the mirror surface, including those undergoing a previous or subsequent deflection from the adsorbate, with incident wave vector $\mathbf{k}_s$. Because of the spherical geometry of the investigated model, the angular distribution spanned by Eq. (1) can be characterized exactly from a single 1D numerical resolution for an arbitrary scatterer-adsorbate potential [13,15]. This exact scattering formulation for a hemisphere model [13,15] was initially proposed to reproduce total (vs differential) cross sections. The authors of Refs. [13,15] revealed that the van der Waals attraction was most important for quantitative comparison with experimental data and a gas phaselike glory effect [1,2] was evidenced [13]. The purpose of the present investigation is to apply this theory to characterize the richer patterns of the differential cross section.

Within the hard wall model, the gas phase scattering amplitude can be formulated analytically as a function of the hard sphere radius a, e.g., Eq. (23) of Ref. [12]. The reflection construction of Eq. (1) for the hard hemisphere model then yields [14,16]

$$F^{\mathrm{HH}}(\mathbf{k}_f, \mathbf{k}_i) = \frac{i}{k_i} \sum_{\ell=1}^{\infty} (2\ell + 1) \frac{j_\ell(k_i a)}{h_\ell(k_i a)} \times [P_\ell(\mathbf{k}_f \cdot \mathbf{k}_i) - P_\ell(\mathbf{k}_f \cdot \mathbf{k}_s)], \qquad (2)$$

in terms of the spherical Bessel and Hankel functions j_ℓ and h_ℓ, and of the Legendre polynomial P_ℓ [17]. For in-plane scattering, as in the experiments of Toennies and coworkers [5–7], Eq. (1) translates as $F(\mathbf{k}_f, \mathbf{k}_i) = f(\pi - \theta_i - \theta_f) - f(\theta_f - \theta_i)$, where θ is the angle between $\mathbf{k}$ and the normal to the surface. In order to compare to the CL calculations performed under normal incidence, the latter expression can be simplified such as $F(\mathbf{k}_f, \mathbf{k}_i) = f(\pi - \theta_f) - f(\theta_f)$, which reduces Eq. (2) to

$$F^{\mathrm{HH}}(\mathbf{k}_f, \mathbf{k}_i) = -\frac{2i}{k_i} \sum_{\ell=\mathrm{odd}} (2\ell + 1) \frac{j_\ell(k_i a)}{h_\ell(k_i a)} P_\ell(\cos\theta_f). \qquad (3)$$

The hard sphere scattering amplitude can be further decomposed into two contributions, namely, the backscattering or illuminated face term and the Fraunhofer term [5,7]. It may be instructive to isolate the Fraunhofer contribution since it is predominant in the forward scattering from a hard wall. By specializing the analytical formula given by Eq. (4) of Ref. [7] to the case of normal incidence, the reflection construction leads to

$$F^{F}(\mathbf{k}_f, \mathbf{k}_i) = ia \cot(\theta_f) J_1(k_i a \sin\theta_f), \qquad (4)$$

in terms of the cylindrical Bessel function J_1 [17].

After the scattering dynamics review it remains to define the interaction potential for the soft hemisphere model. Figure 1 displays a contour plot of the He-CO/Pt(111) potential referred to as model I by CL, as a function of the distance to the surface, z, and of the distance from the adsorbate along the surface, ρ. It consists of the sum of a Morse potential for the He interaction with the flat surface, and of an isotropic Lennard-Jones potential for the gas phase He-CO interaction [8], hereafter denoted by $V_{\mathrm{Pt(111)}}$ and V_{CO}, with well depths of 4.0 and 2.37 meV, respectively. Because this soft potential closely approximates a hemisphere geometry as can be seen in Fig. 1, the comparison between the reference calculations of CL and the reduced-dimensionality treatments stemming from the hemisphere models will unambiguously assess the relevance of the latter simplified descriptions. In other words, the predictive power of the hemisphere descriptions is obviously expected to weaken as one attempts to interpret experimental observations.

Figure 2 shows the $V_{\mathrm{Pt(111)}}$ and V_{CO} potential curves and those for He scattering directly above the adsorbed CO, $V_{\mathrm{CO+Pt(111)}} = V_{\mathrm{CO}} + V_{\mathrm{Pt(111)}}$ with well depth of 2.96 meV, and for a purely repulsive, V_{CO}-based interaction. The difference between $V_{\mathrm{CO+Pt(111)}}$, that is,

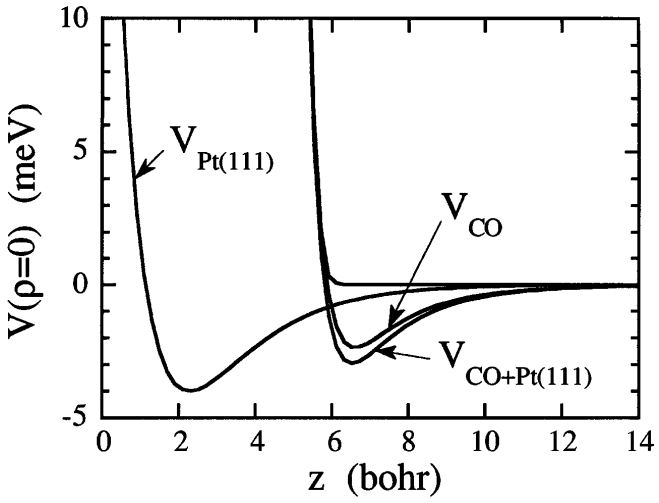

FIG. 2. Potential energy curves for He scattering from Pt(111) and from various CO sphere models: Adsorbed, free, and purely repulsive.

for $\rho = 0$ in Fig. 1, and $V_{\mathrm{Pt(111)}}$, that is, roughly for $\rho = 8$ bohr in Fig. 1, represents the magnitude of the corrugation induced by the presence of the isolated CO adsorbate. The collision energy range spanned by CL is centered about 10 meV, i.e., 6–14 meV. The 10 meV equipotential from Fig. 1 yields $r = 5.40$ and 5.34 bohr, for $\rho = 0$ and 5 bohr, respectively, with $r^2 = \rho^2 + z^2$. This confirms that the He probes an adsorbed hemisphere, only slightly distorted by the surface interaction, on one hand, and it gives an estimate of a for the hard sphere calculations, on the other hand.

Figure 3 displays the 10 meV angular distributions obtained within three distinct hemisphere models, namely,

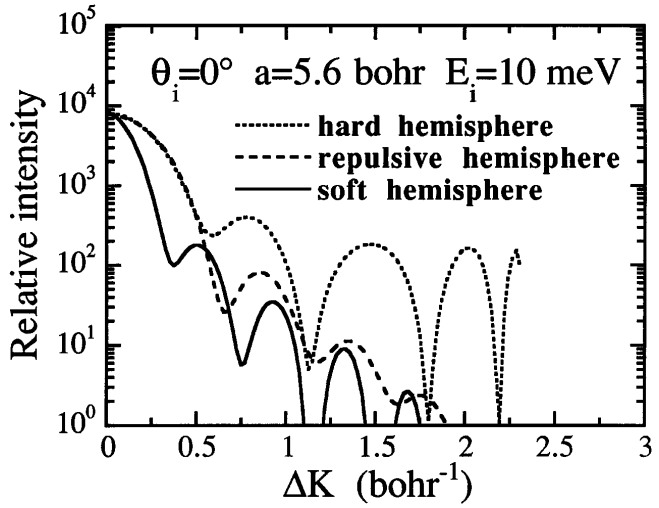

FIG. 3. Differential cross sections as a function of parallel momentum transfer, for He scattering with a collision energy of 10 meV from an adsorbed hemisphere under normal incidence. The solid, dashed, and dotted curves refer to the attractive, purely repulsive, and hard wall interactions, respectively. The hard radius is $a = 5.6$ bohr.

the $V_{\mathrm{CO+Pt(111)}}$ soft, V_{CO}-based purely repulsive and hard wall ($a = 5.6$ bohr) interactions, respectively. It is found that the hard hemisphere differential cross sections do not change appreciably when the hard sphere radius is increased from 5.3 to 5.6 bohr. In addition, replacing $V_{\mathrm{CO+Pt(111)}}$ with V_{CO} does not significantly shift the interference maximum locations. CL found the positions of the three first maxima away from specular reflection to be $\Delta K_1 = 0.48$, $\Delta K_2 = 0.91$, and $\Delta K_3 = 1.34$, ± 0.02 bohr^{-1}, within model I. Remarkably, the soft hemisphere model reproduces these results, i.e., $\Delta K_1 = 0.50$, $\Delta K_2 = 0.92$, and $\Delta K_3 = 1.33$. Upon comparing the dotted and solid lines it is obvious that the hard hemisphere model fails to interpret the CL results. A better match can be obtained, i.e., $\Delta K_1 = 0.48$, $\Delta K_2 = 0.89$, and $\Delta K_3 = 1.39$, if one assumes the hard radius to be $a = 9.6$ bohr which is truly unrealistic in view of the contour plot depicted in Fig. 1. Moreover, the agreement cannot remain satisfactory if one considers any other energy 6, 8, 12, 14 meV probed in that range, because the hard hemisphere calculations result in an erratic dependence of the peak positions as a function of incidence energy for a given value of a (not shown here). In contrast, the soft hemisphere calculations define fixed positions versus the incidence energy in the range 6–14 meV, within ± 0.02 bohr^{-1} for ΔK_1 and ΔK_2, in very good agreement with CL. ΔK_3 is slightly more sensitive to the collision energy, especially at low energy, decreasing from 1.36 bohr at 14 meV down to 1.26 bohr at 6 meV, the agreement with CL remaining quite good overall. The dashed line in Fig. 3 shows the effect of removing the potential well in the He-adsorbate interaction. Although it is well known from gas phase scattering that the van der Waals well causes the rainbow effect that evolves as a remnant shoulder at high energies (see Fig. 1 of Ref. [3]) the vanishing of the first interference maximum within the purely repulsive hemisphere model unambiguously elucidates the nature of this peak. In addition, the three dashed interference peaks closely correspond to the oscillations following the soft hemisphere rainbow, whereas they strongly depart from the hard wall oscillatory structure, perhaps with the exception of the first maximum. This demonstrates that the hard hemisphere model cannot even account for diffraction effects, at least for these low incidence energies. Surprisingly, the pure Fraunhofer model of Eq. (4) ideally reproduces ΔK_2 at all energies with $a = 5.6$ bohr, as already found by CL, because reflection symmetry interferences appear to have no sizable effect. It does not seem to be a mere coincidence since it also occurred for model II [9].

Figure 4 compares the angular distributions stemming from the adsorbed hemisphere and gas phase sphere models, and thereby illustrates the role of the reflection symmetry interferences. The solid and dotted lines, respectively, correspond to $F(\mathbf{k}_f, \mathbf{k}_i)$ and $f(\mathbf{k}_f \cdot \mathbf{k}_s)$ of Eq. (1), the $f(\mathbf{k}_f \cdot \mathbf{k}_i)$ contribution being roughly constant. There is a perfect qualitative match of the two interference patterns at the exception of the small

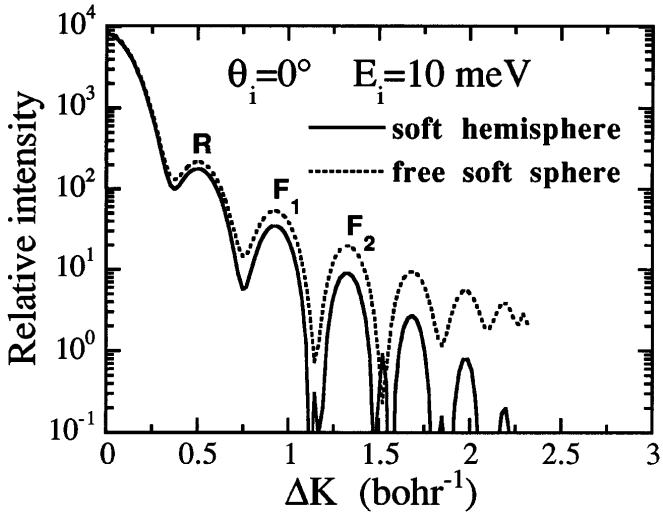

FIG. 4. Differential cross sections as a function of momentum transfer, for He scattering with a collision energy of 10 meV from an adsorbed soft hemisphere under normal incidence (solid curve) and from a free soft sphere (dotted curve). R labels the rainbow, and F_1 and F_2 denote the two first Fraunhofer diffraction peaks.

spikes arising at the secondary minima locations of the free sphere distribution, thus featuring the effect of the reflection symmetry interferences. In view of the fairly weak intensity of these spikes one can conclude that they must be negligible in the 3D scattering distribution, the largest one buried in the overlapping interference structure of the F_3 diffraction peak and R_2 surface-specific rainbow, such as depicted in Fig. 4 of Ref. [9].

A few summarizing remarks are in order. Starting with negative statements, this study has shown that the hard hemisphere model completely fails to interpret the 3D scattering calculations that are based on an adsorbate interaction closely reproducing a hemisphere geometry. One might expect the hard wall model to be more relevant at higher collision energies, but this can be denied as well in view of the poor agreement with the purely repulsive, nonhard hemisphere model. Next, the reflection symmetry interferences are found to play a minor, indeed negligible role in the 3D scattering distribution. The main positive information brought by this work is threefold. First, the proposed soft hemisphere model perfectly predicts the first three interference peaks denoted by R, F_1, and F_2 in Fig. 4. Second, the first interference maximum, R, previously misinterpreted as a diffractionlike peak [5–9,11], is revealed as the well-known gas phase rainbow arising from the van der Waals interaction between the scatterer and the adsorbate. It is expected to occur even at higher energies and may well be already observable in the experimental angular distributions as a remnant shoulder (see the figures of Ref. [7] and Fig. 3 of Ref. [11]). Lastly, every feature of the 3D scattering distribution (see Fig. 4 of Ref. [9]) can now be unambiguously assigned. As parallel momentum transfer increases the differential cross section is characterized by a gas phaselike rainbow (R), two Fraunhofer diffraction maxima (F_1 and F_2), and two surface-specific rainbows, a single collision, and a double collision event, respectively. Of course, the last two features evidenced by Yinnon, Kosloff, and Gerber [8] cannot be reproduced by a hemisphere model lacking in the surface-induced distortion mechanism responsible for these rainbows.

The future perspectives of this study are to extend the soft hemisphere calculations to compare with the high-resolution experimental data recently obtained for He-CO/Cu(100) [7], as well as with exact scattering distributions stemming from a more realistic interaction potential, e.g., with an elongated shape along the surface normal. Last, the future investigation should span the experimental range of beam energies, that is, 10–50 meV. This would clarify whether the surface-induced rainbows rather than the hemisphere features, are amplified with increasing energy as indicated by Yinnon, Kosloff, and Gerber [8].

*Email address: didier.lemoine@univ-lille1.fr

†The Centre d'Etudes et de Recherches Laser et Applications is supported by the Ministère chargé de la Recherche, the Région Nord/Pas de Calais, and the Fonds Européen de Développement Economique des Régions.

[1] H. Pauly, in *Atom-Molecule Collision Theory*, edited by R. B. Bernstein (Plenum, New York, 1979).
[2] R. D. Levine and R. B. Bernstein, *Molecular Reaction Dynamics and Chemical Reactivity* (Oxford University, New York, 1989).
[3] L. Beneventi, P. Casavecchia, and G. G. Volpi, J. Chem. Phys. **85**, 7011 (1986).
[4] R. T. Pack, Chem. Phys. Lett. **55**, 197 (1978).
[5] A. M. Lahee, J. R. Manson, J. P. Toennies, and Ch. Wöll, J. Chem. Phys. **86**, 7194 (1987).
[6] M. Bertino, J. Ellis, F. Hofmann, J. P. Toennies, and J. R. Manson, Phys. Rev. Lett. **73**, 605 (1994).
[7] A. P. Graham, F. Hofmann, J. P. Toennies, and J. R. Manson, J. Chem. Phys. **105**, 2093 (1996).
[8] A. T. Yinnon, R. Kosloff, and R. B. Gerber, J. Chem. Phys. **88**, 7209 (1988).
[9] M. N. Carré and D. Lemoine, J. Chem. Phys. **101**, 5305 (1994).
[10] C. W. Skorupka and J. R. Manson, Phys. Rev. B **41**, 9783 (1990).
[11] B. H. Choi, K. T. Tang, and J. P. Toennies, J. Chem. Phys. **107**, 1631 (1997).
[12] B. H. Choi, K. T. Tang, and J. P. Toennies, J. Chem. Phys. **107**, 9437 (1997).
[13] H. Jónsson, J. H. Weare, and A. C. Levi, Surf. Sci. **148**, 126 (1984); Phys. Rev. B **30**, 2241 (1984).
[14] M. Heuer and T. M. Rice, Z. Phys. B **59**, 299 (1985).
[15] S. D. Bosanac and M. Sunjic, Chem. Phys. Lett. **115**, 75 (1985).
[16] D. Lemoine, J. Chem. Phys. (to be published).
[17] M. Abramowitz and I. A. Stegun, *Handbook of Mathematical Functions* (Dover, New York, 1970).